NASA Technical Memorandum 83551

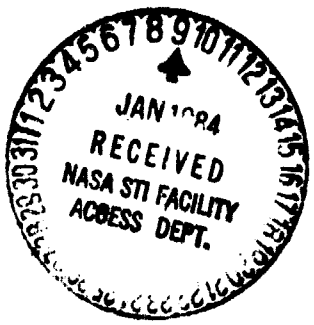

Particulate Erosion Mechanisms

P. Veerabhadra Rao and Donald H. Buckley
Lewis Research Center
Cleveland, Ohio

Prepared for the
Cavitation and Multiphase Flow Forum
sponsored by the American Society of Mechanical Engineers
New Orleans, Louisiana, February 11-17, 1984

NASA

PARTICULATE EROSION MECHANISMS

P. Veerabhadra Rao[1] and Donald H. Buckley
National Aeronautics and Space Administration
Lewis Research Center
Cleveland, Ohio 44135

ABSTRACT

Particulate damage and erosion of ductile metals are today plaguing design and field engineers in diverse fields of engineering and technology. It has been found that too many models and theories have been proposed leading to much speculation from debris analysis and failure mechanism postulations. Most theories of solid particle erosion are based on material removal models which do not fully represent the actual pnysical processes of material removal. The various mechanisms proposed thus far have been: melting, low-cycle fatigue, extrusion, delamination, shear localization, adhesive material transfer, etc. This paper presents the experimental data on different materials highlighting the observed failure modes of the deformation and cutting wear processes using optical and scanning electron microscopy. This paper also addresses the most important mechanisms proved from the experimental observations of the specimens exposed to both spherical and angular particles, and discusses the validity of the earlier theories. Both the initial stages of damage and advanced stages of erosion were studied to gain a fundamental understanding of the process.

INTRODUCTION

The solid particulate erosion of ductile metals has been attributed to different mechanisms such as hardening and embrittlement [1], extrusion [2], melting [3], low cycle fatigue [4], adhesive material transfer [5] and shear localization [6]. In addition, fracture of the particles with radial outflow of fragments [7], delamination of subsurface [8] and ductile fracture [9] have also been postulated. Several possible mechanisms of the material debris removal have been explained by different investigators [10 to 13] using angular and spherical erodent particles for normal and oblique impingement conditions. Finnie et al., [9] recently stated that they favor an extrusion process ending in ductile fracture, but not completely excluding "low cycle fatigue" or "delamination wear" as potential mechanisms. Although there exists a substantial amount of recent literature to support various mechanisms, it is rather difficult to interpret a universal mechanism using both spherical and angular particles at different angles of impingement. This may be due partly to the fact that the spherical particle impingement induces "deformation wear" resulting in "flake-type" debris and the angular particle impingement induces "cutting wear" resulting in "angular, cut-faceted" surfaces.

This study reports some recent observations with regard to material removal mechanisms using both angular and spherical particles at normal incidence.

EXPERIMENTAL APPARATUS AND PROCEDURE

Materials

Specimens of 6061-T6 aluminum alloy, copper, 1045 steel, A108 steel, and 4340 steel were used in this investigation. The specimens were 6 mm thick, 25 mm wide, and 37.5 mm long. Before exposure to glass bead and crushed glass impingement, all specimens were polished with 600-grit emery paper, then with 3 μm diamond paste, cleaned with distilled water, and air dried.

Experimental Apparatus and Procedure

A sandblasting facility was used to continuously impact test specimens at normal incidence. Spherical glass beads of 20 μm average diameter and crushed glass of 30 μm average size were used. In the sandblasting facility the distance between the specimen and nozzle (1.18 mm diam) was 13 mm. Argon was used as the driving gas.

The damaged and eroded surfaces were observed with optical and scanning electron microscopes, and chemical analyses were obtained by means of energy dispersive x-ray spectroscopy (EDS).

RESULTS AND DISCUSSION

Damage During Initial Stages

Figure 1 presents photographs of etched 6061-T6 aluminum alloy, OFHC copper and 1045 steel surfaces exposed for 2 sec to 52 m/s velocity crushed glass

---

[1]Cleveland State University, Cleveland, Ohio 44115.

jet. Photographs in Fig. 1 show the transition from inception to complete damage of the grain structure. The particles embedded on the surface indicate preferential grain boundary attack which was not observed earlier [14]. The embedment of particles are maximum at the grain boundary. Ductile tearing appears but grain boundary opening up was not observed [14] during crushed glass impingement as indicated in Fig. 2, even at an advanced stage of erosion. Strain and strain hardened layers were observed in this study. The explanation for the strain hardened layer formation by Salik et al [5] for single and multiple particle impact and the "extrusion type" model proposed by Hutchings and Cousens [13] have some bearing on the observation. The repeated impacts induce strain hardening of the material surface before fatigue-type failure takes place.

Although extensive slip band formation was noticed for copper specimens at higher magnifications (Fig. 1(b)), the glide band structures as reported by Ives and Ruff [10] were not observed. Both fine lamellar pearlite (dark) and ferrite (white) areas on the 1045 steel surface (Fig. 1(c)) were attacked equally. In some instances, however, ferrites appear to be attacked more.

Figure 3 shows SEM micrographs of 4340 steel surfaces at the inception stages during glass bead and crushed glass impingement. The grain boundary damage and tilting are seen in both cases; the structure, however, was completely damaged as indicated in Fig. 3(b) during crushed glass impingement. The debris found on both surfaces was photographed to observe the form (size and shape) and type of particle removal process. The initial debris appears to be as dust (for glass bead impingement) and cut, faceted and angular particles (for crushed glass impingement). Different sizes and shapes of particles have been reported in the literature during solid particle impingement [15]. Brown and Edington [16] observed that copper at the surface was lost by (1) melting, (2) dusting, and (3) sheet formation processes. The surface melting is, however, not observed on aluminum alloy, copper and steel. Further, studies with Pb and In indicated that both flow of material and melting are possible with both forms of glass [17]. This supports the earlier postulation that melting of surfaces takes place [3, 16 and 18]. There appears to be a threshold energy (size of particle or velocity of impact) necessary to cause melting during solid particle erosion.

Further, it may be stated that in order to observe melting it appears necessary to (1) increase the impact velocity, (2) increase the particle size, (3) keep the angle of impact at maximum erosion conditions, or (4) adopt a low melting point metal.

It is generally believed that high repetitive impact forces between a surface and an abrasive particle lead to plastic deformation and fracture. When erodent particles strike a surface at an oblique or normal angle under a sufficient contact stress (or force) they "plow" or "cut" the surface depending on the shape of particles. Figure 4 shows individual craters on aluminum alloy surfaces during the very early stages of glass bead impingement. There is sufficient evidence to support, plastic deformation, repeated impact, final "fatigue-type" and "extrustion-type" failures. However, if the phenomenon is observed with respect to time or the intensity of erosion, different mechanisms (melting, fatigue, extrusion, shear localization, adhesive material transfer[2], delamination, and so on) may be seen as individual processes dominating erosion. Despite the fact that individual flakes are being removed by repeated impact and final "fatigue-type" failure, the typical striations during conventional fatigue failure are, however, not observed.

Erosion During Advanced Stages

Figure 5 presents cross-sectional views of an aluminum alloy, copper and 1045 steel specimen surfaces after 10 min exposure to 100 m/s velocity glass bead jet impingement. The advanced stages of erosion have been specifically chosen in order to understand some specifics of erosion mechanism at the subsurface which is not seen at the inception stages of damage. In Fig. 5(a), (aluminum alloy), origin of subsurface damage is observed and cracking extends approximately up to 120 μm deep. Cracking appears not to occur in any preferential direction in a majority of cases. This mechanism may be anticipated due to the maximum shear stress occurring at subsurface during impingement. The initiated crack beneath the surface radiates to the surface or joins with the adjacent cracks to remove material. In light of high-stress incident on the surface, this type of subsurface cracking and surface fatigue damage are anticipated. In this particular case, the "delamination theory" proposed by Suh [8] and "shear localization theory" proposed by Shewmon [6] appear to be significant. It is rather strange that Figs. 5(b) (copper) and 5(c) (1045 steel) do not show any subsurface damage. One may anticipate at this juncture that copper and 1045 steel may still require higher particle sizes and velocities in order to cause observed subsurface damage. Further, photographic observations indicate that surface cracks initiate at grain boundaries for copper which is not a general damage feature.

Debris Analysis

Figure 6 presents debris collected after glass bead impingement on A108 steel surface observed in ferrographic analysis. The shapes vary from dust, "needle type," flakes to spherical particles. The size generally varies from 0.1 to 5 μm. Ruff [15] reported a size range from 1 to 5 μm for 1015 steel during Al_2O_3 angular particle impingement. Brown and Edington [16] mentioned 0.1 to 1 μm for irregular globular particles and 0.1 to 5 μm (and about 0.02 μm thick) for thin sheets (not platelets) during spherical SiC particle impingement on polycrystalline aluminum specimens. Spherical debris formation was also reported by Andrews and Field [19] during steel sphere impact on the surface of copper specimens. Dust observed on the surface of 4340 steel (Fig. 3(a)) also support the present observation. Flakes [12] and angular particles [14] have been reported by the present investigators earlier using 6061-T6 aluminum alloy.

The formation of different shapes of particles may be attributed to the following different mechanisms: Dust - (1) fracture of top layers during repeated im-

[2]It was observed during the erosion process that at near glancing angles to maximum erosion conditions (<25 deg) the erodents changed color from white to dark brown and then to black indicating adhesive material transfer and chemical activity similar to that observed on the material surfaces earlier [12].

pact, (2) adhesive material transfer during rebound phase of particles, and (3) extrusion (splashing as well as possible melting) of the metal. Spherical particles - (1) splashing and possible local melting, and (2) extrusion of the metal during cutting and removal processes. Flake type particles - (1) repeated impact and final "fatigue-type" failure, and (2) "shear localization" and "delamination."

The different sizes and shapes of particles are believed to provide clues to assess the mechanisms involved during the erosion process and also to furnish guidance for the theoretical modeling efforts. Hence, it is necessary to collect the debris in a systematic way in order to further understand the mechanism inherent in different stages of erosion. It is also necessary, from a fundamental erosion point of view, to fully understand the observed good correlations of surface energy, strain energy and atomic volume with erosion rates [17].

CONCLUSION

In conclusion, ductile metal erosion appears to be dominated with "extrusion," "fatigue-type failure," "delamination," and "shear localization." Melting, adhesive material transfer and cutting also play important roles depending upon individual parameters of particles such as the velocity of impact and the size, shape and concentration of the erodent. At present it appears that all mechanisms may not be observed at a given individual experimental condition. It is now clear that two or three different mechanisms can fully explain the erosion process at any experimental stage with angular and spherical particles. The interrelation between different mechanisms is essential for future assessment. It is further necessary, from a fundamental erosion point of view, to fully understand the observed good correlation of surface energy, strain energy and atomic volume with erosion rates.

REFERENCES

1. Bitter, J. G. A., "A Study of Erosion Phenomena, Parts I and II," Wear, vol. 6, 1963, pp. 5-21 and 169-190.
2. Sheldon, G. L., and Kanhere, A., "An Investigation of Impingement Erosion Using Single Particles," Wear, vol. 21, 1972, pp. 195-209.
3. Smeltzer, C. E., Gulden, M. E., and Compton, W. A., "Mechanisms of Metal Removal by Impacting Dust Particles," ASME Journal of Basic Engineering, vol. 92, no. 3, Sept. 1970, pp. 639-654.
4. Finnie, I., "Some Observations on the Erosion of Ductile Metals," Wear, vol. 19, Jan. 1972, pp. 81-90.
5. Salik, J., and Brainard, W. A., "Adhesive Material Transfer in the Erosion of an Aluminum Alloy," NASA TM-79165, 1979; Salik, J., Buckley, D. H., and Brainard, W. A., "The Effect of Mechanical Surface and Heat Treatments on the Erosion Resistance of 6061 Aluminum Alloy," Wear, vol. 65, Jan. 1, 1981, pp. 351-358.
6. Christman, T., and Shewmon, P. G., "Adiabatic Shear Localization and Erosion of Strong Aluminum Alloys," Wear, vol. 54, May 1979, pp. 145-155; Sundararajan, G., and Shewmon, P. G., "A New Model for the Erosion of Metals at Normal Incidence," Wear, vol. 84, no. 2, Jan. 15, 1983, pp. 237-258.
7. Tilly, G. P., "A Two Stage Mechanism of Ductile Erosion," Wear, vol. 23, Jan. 1973, pp. 87-96.
8. Suh, N. P., "The Delamination Theory of Wear," Wear, vol. 25, 1973, pp. 111-124.
9. Ives, L. K., and Ruff, A. W., "Electron Microscopy Study of Erosion Damage in Copper," Erosion: Prevention and Useful Applications, W. F. Adler, ed., ASTM STP 664, American Society for Testing and Materials, Philadelphia, 1979, pp. 5-35.
10. Brown, R., Jun, E. J., and Edington, J. W., "Erosion of α-Fe by Spherical Glass Particles," Wear, vol. 70, no. 3, Aug. 15, 1981, pp. 347-363.
11. Rao, P. V., Young, S. G., and Buckley, D. H., "Morphology of Ductile Metals Eroded by a Jet of Spherical Particles Impinging at Normal Incidence," Wear, vol. 85, Mar. 1, 1983, pp. 223-237.
12. Cousens, A.K., and Hutchings, I. M., "A Critical Study of the Erosion of an Aluminum Alloy by Solid Spherical Particles at Normal Impingement," Wear of Materials 1983, K.C. Ludema, ed., American Society of Mechanical Engineers, New York, 1983, pp. 382-389.
13. Finnie, I., Levy, A., and McFadden, D. H., "Fundamental Mechanisms of the Erosive Wear of Ductile Metals by Solid Particles," Erosion: Prevention and Useful Applications, W. F. Adler, ed., ASTM STP 664, American Society for Testing and Materials, Philadelphia, 1979, pp. 36-58.
14. Rao, P. V., Young, S. G., and Buckley, D. H., "Morphology of an Aluminum Alloy Eroded by a Normal Incidence Jet of Angular Erodent Particles," Wear, vol. 92, no. 1, 1983, pp. 31-49.
15. Ruff, A. W., "Debris Analysis of Erosive and Abrasive Wear," Fundamentals of Tribology, N. P. Suh and N. Saka, eds., MIT Press, Cambridge, 1980, pp. 877-885.
16. Brown, R., and Edington, J. W., "Mechanisms of Material Loss During the Threshold Period of Erosion by Solid Particles," Wear, vol. 77, no. 3, Apr. 15, 1982, pp. 347-353.
17. Rao, P. V., and Buckley, D. H., "Solid Impingement Erosion Mechanisms and Characterization of Erosion Resistance of Ductile Metals," NASA TM-83492, 1984.
18. Brown, R., and Edington, J. W., "The Melting of Metal Targets During Erosion by Hard Particles," Wear, vol. 71, no. 1, Sept. 1, 1981, pp. 113-118.
19. Andrews, D. R., and Field, J. E., "Temperature Dependence of the Impact Response of Copper: Erosion by Melting," Journal of Physics D: Applied Physics, vol. 15, 1982, pp. 2357-2367.

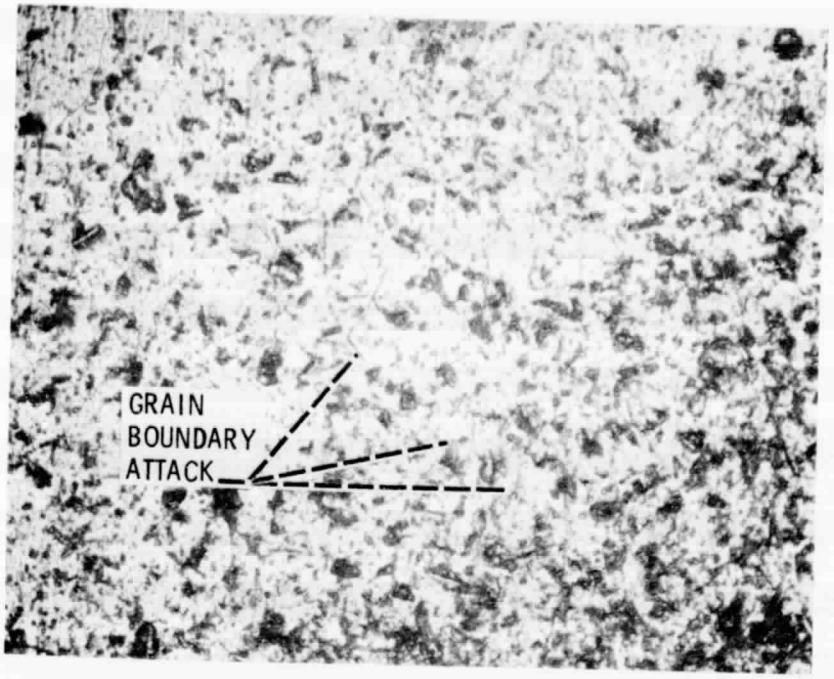

(a) 6061-T6 aluminum alloy, (etchant, 2% HF + H_2O).

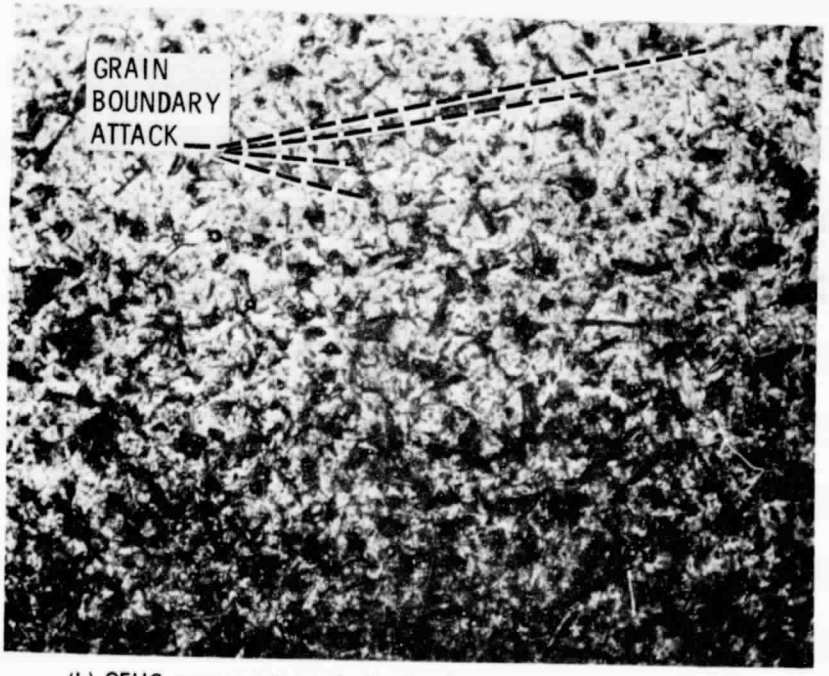

(b) OFHC copper (etchant, $K_2Cr_2O_7 + H_2SO_4 + HCl + H_2O$).

Figure 1. - Photographs depicting grain damage after crushed glass impingement. Average particle velocity, 52 m/s; Crushed glass flow, 0.34 g/s.

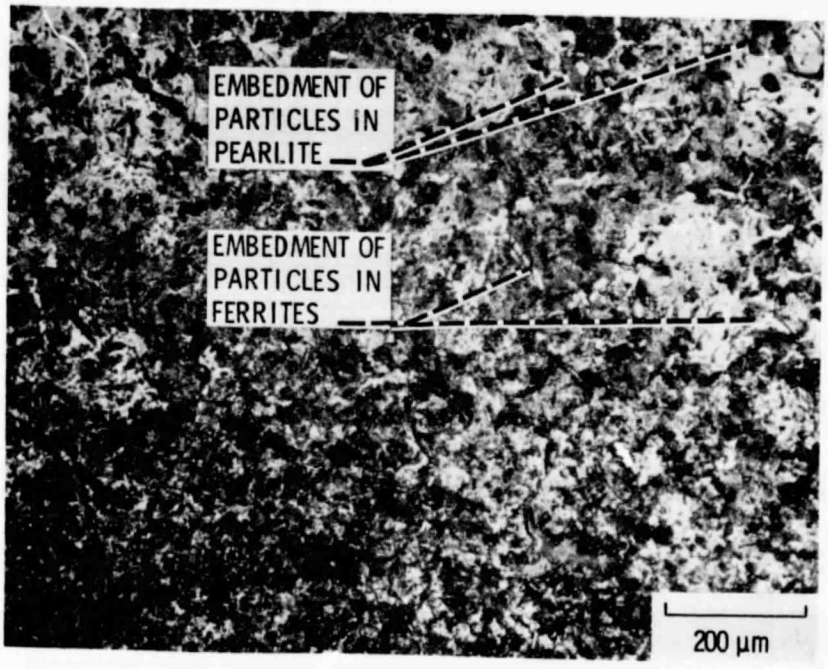

(c) 1045 steel (etchant, 4% Nital).

Figure 1. - Concluded.

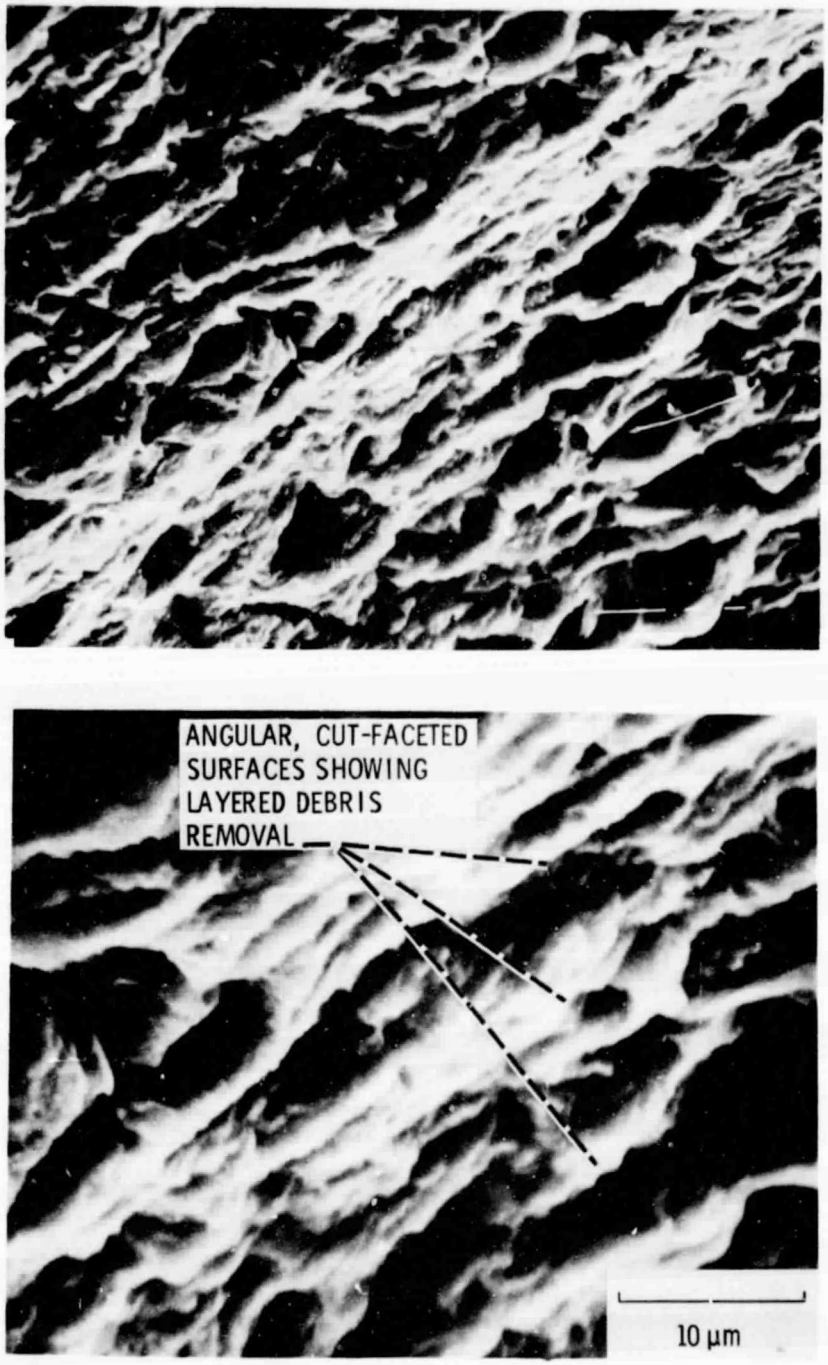

Figure 2. - SEM micrographs of aluminum alloy surfaces during cutting (cut, faceted appearance) wear process depicting false grain boundary opening up. Average particle velocity, 68 m/s; Crushed glass flow, 0.25 g/s; Exposure time, 10 min.

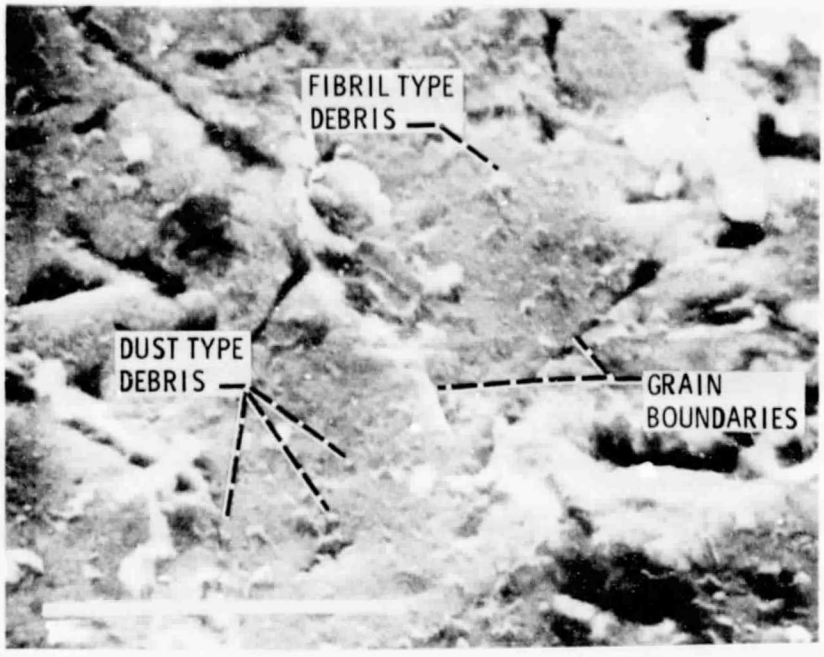

(a) Glass bead impingement.

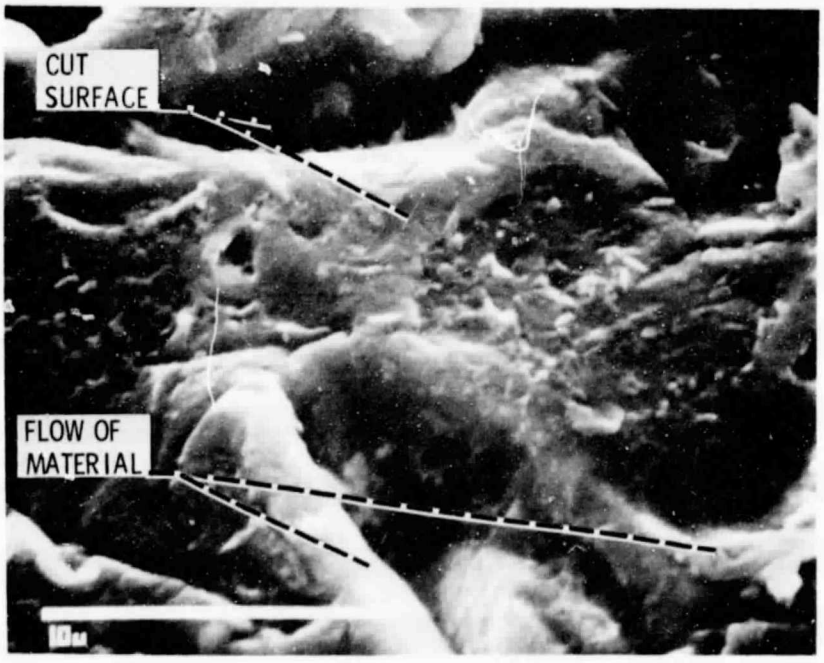

(b) Crushed glass impingement.

Figure 3. - SEM micrographs of grain damage on 4340 steel surfaces during glass bead and crushed glass impingement. Average particle velocity, 52 m/s; Exposure time, 2 sec; Etchant, 4% Nital.

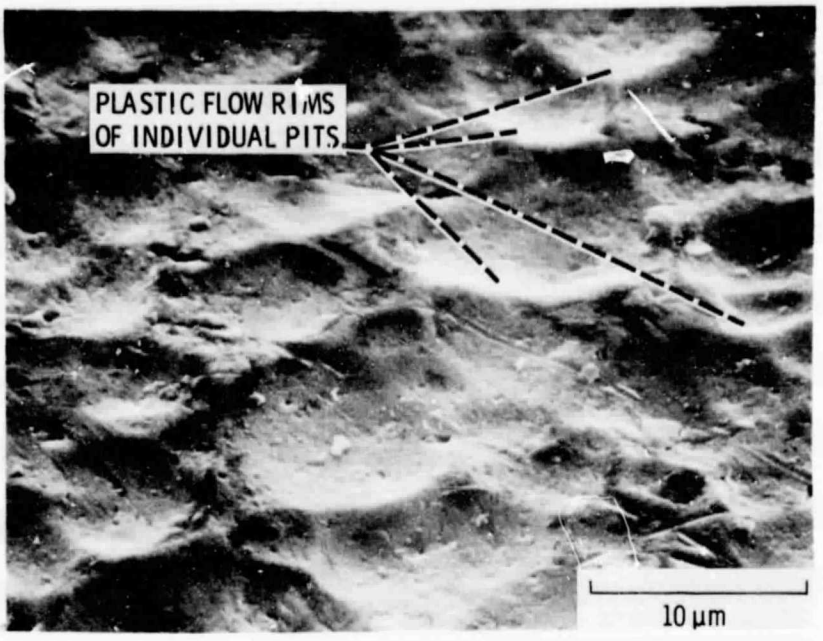

(a) Individual impacts with lips of plastically displaced metal and distorted as well as deformed surface layers.

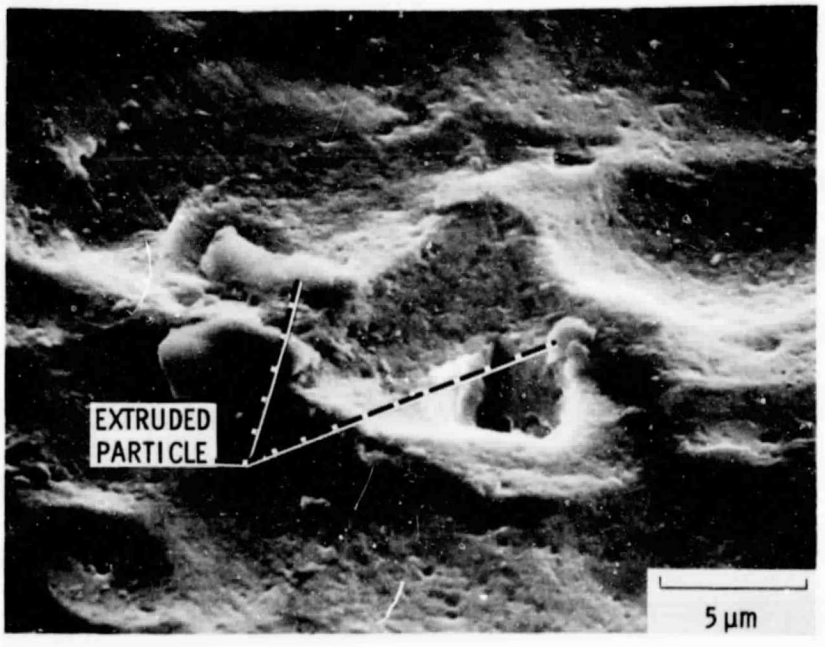

(b) Extrusion of particles.

Figure 4. - SEM micrographs of individual dents on aluminum alloy surface. Average particle velocity, 100 m/s; Exposure time, 2 s; Glass bead flow, 0.75 g/s.

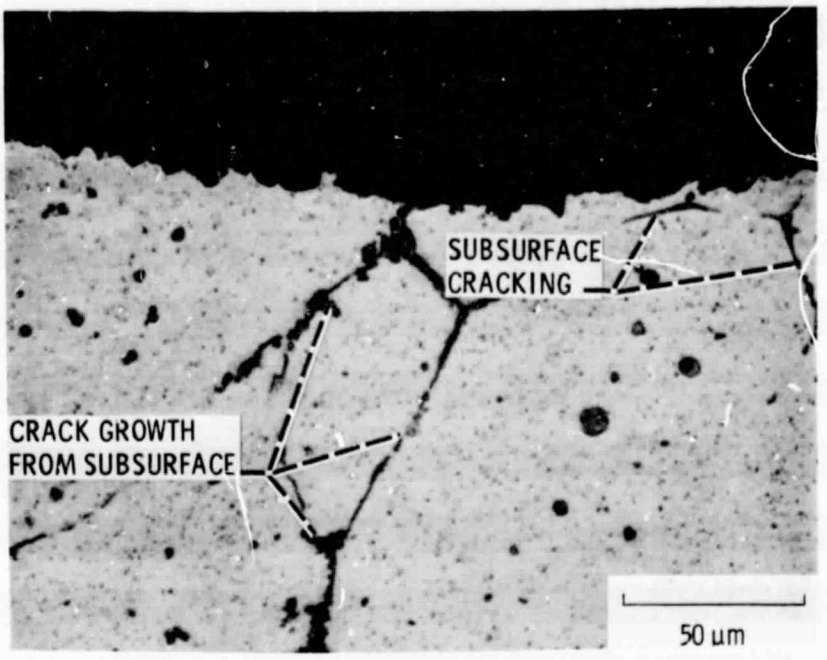

(a) 6061-T6 aluminum alloy.

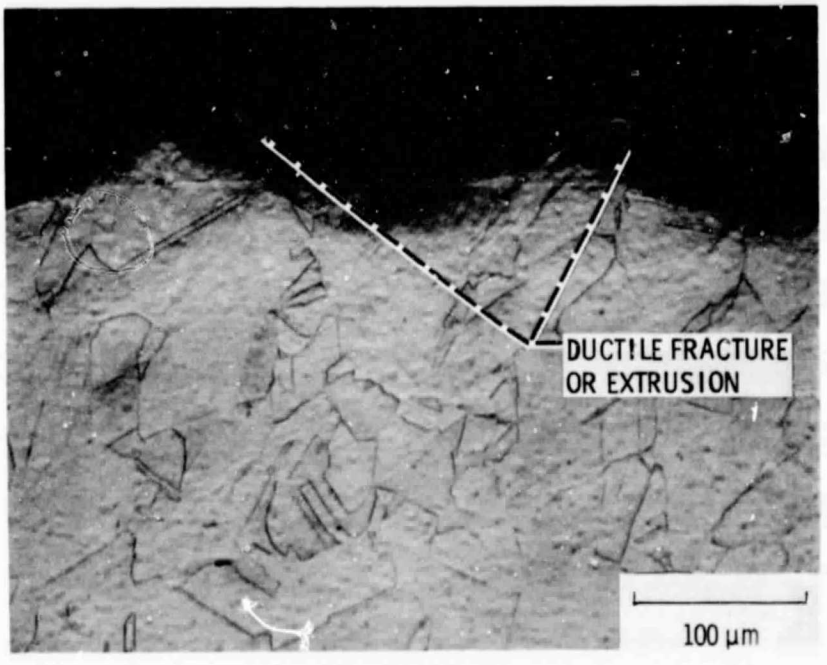

(b) OFHC copper.

Figure 5. - Photographs of cross sections of eroded specimens during glass bead impingement. Average particle velocity, 100 m/s; Exposure time, 10 min; Glass bead flow, 0.75 g/s.

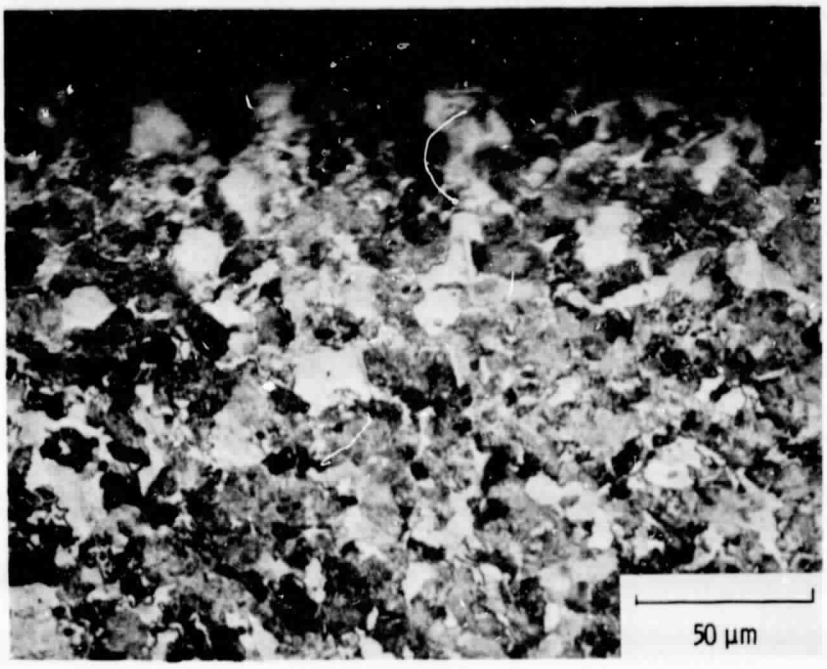

(c) 1045 steel.

Figure 5. - Concluded.

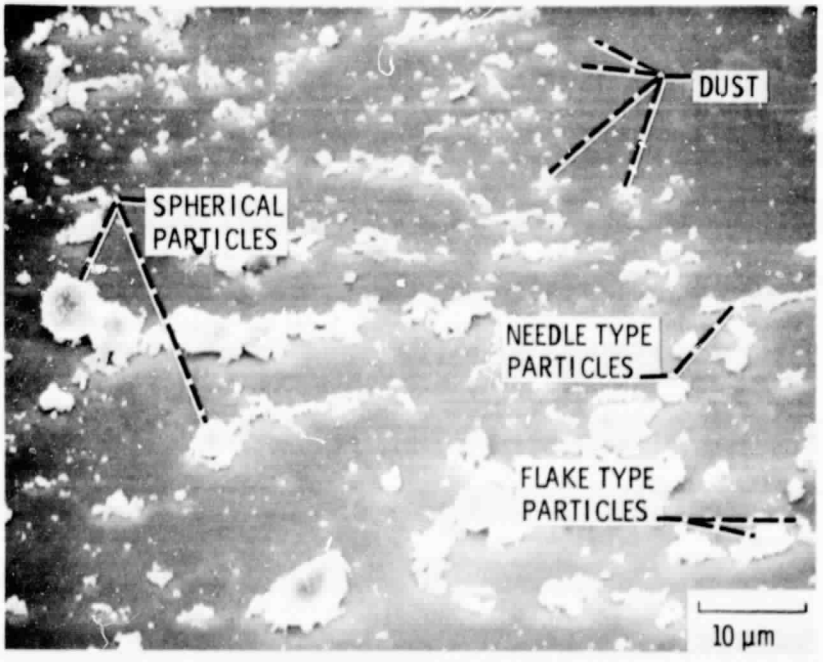

Figure 6. - Different shapes and sizes of particles observed in ferrographic analysis.